

# Molecular Mechanisms of TLR2-Mediated Antigen Cross-Presentation in Dendritic Cells

Kuan-Yin Shen,<sup>\*,†</sup> Ying-Chyi Song,<sup>†</sup> I-Hua Chen,<sup>†</sup> Chih-Hsiang Leng,<sup>†,‡</sup> Hsin-Wei Chen,<sup>†,‡</sup> Hui-Ju Li,<sup>†</sup> Pele Chong,<sup>†,‡</sup> and Shih-Jen Liu<sup>\*,†,‡</sup>

Cross-presentation is a key function of dendritic cells (DCs), which present exogenous Ags on MHC class I molecules to prime CTL responses. The effects of TLR triggering on the cross-presentation of exogenous Ags by DCs remain unclear. In this study, we used synthetic dipalmitoylated peptides and TLR2 agonist-conjugated peptides as models to elucidate the mechanisms of TLR2-mediated cross-presentation. We observed that the internalization of dipalmitoylated peptides by bone marrow-derived DCs was facilitated by TLR2 via clathrin-mediated endocytosis. The administration of these dipalmitoylated peptide-pulsed bone marrow-derived DCs eliminated established tumors through TLR2 signaling. We further demonstrated that the induction of Ag-specific CTL responses and tumor regression by dipalmitoylated peptides was TAP independent. In addition, presentation of dipalmitoylated peptides by MHC class I molecules was blocked in the presence of an endosomal acidification inhibitor (chloroquine) or a lysosomal degradation inhibitor (Z-FL-COCHO). The endocytosed dipalmitoylated peptide also passed rapidly from early endosome Ag-1-positive endosomes to RAS-related GTP-binding protein 7 (Rab7)-associated late endosomes compared with their nonlipidated counterparts. Furthermore, we found that dipalmitoylated peptide-upregulated Rab7 expression correlated with Ag presentation via the TLR2/MyD88 pathway. Both JNK and ERK signaling pathways are required for upregulation of Rab7. In summary, our data suggest that TLR2-mediated cross-presentation occurs through the upregulation of Rab7 and a TAP-independent pathway that prime CTL responses. *The Journal of Immunology*, 2014, 192: 4233–4241.

The cross-presentation of exogenous Ags is an important biological process that involves the internalization of Ag, trafficking through the endocytic compartment, antigenic peptide generation, and loading of the peptide onto MHC class I molecules. Exogenous Ags are cross-presented by MHC class I molecules through two pathways: 1) the TAP-dependent pathway (or the cytosolic pathway), in which Ags are digested by the proteasome and transported into either the endoplasmic reticulum (ER) (1) or the early endosome (2, 3) for loading onto MHC class I molecules; and 2) the TAP-independent pathway (or the vacuolar

pathway), in which Ags are digested in the endolysosome and directly loaded onto MHC class I molecules (4, 5). The TAP-dependent pathway is associated with proteasomal degradation of cytosolic Ags. The proteasome-generated polypeptides can then be transferred into the ER by TAP1 and TAP2, where these polypeptides must be fine-tuned by ER-associated aminopeptidase 1 for MHC class I loading (6). In the TAP-independent pathway, Ags are digested by cathepsin S, a critical endolysosomal protease, and are then loaded onto MHC class I molecules. Ag processing and loading onto MHC class I molecules occur entirely within the endosome and the acidic lysosomal compartment. Moreover, proteasome-generated polypeptides may be transferred into the endolysosome for MHC class I loading through unknown mechanisms (7). These diverse mechanisms of cross-presentation may arise from different forms of exogenous Ags or may differ among APCs.

A previous study has demonstrated that the cross-presentation of a soluble Ag, OVA, occurs in the early endosomal compartment and that proteasome-dependent degradation is involved in this process (8). Other studies have shown that soluble Ags are cross-presented through the TAP-dependent cytosolic pathway (9, 10) or the TAP-independent vacuolar pathway (4, 10). In particular, Ags conjugated to Abs are targeted to either the early or the late endosome through CD40, the mannose receptor, or DEC205 (11). Efficient cross-presentation is mediated by either prolonged residence of the Ag in the early endosome or decreased degradation in the late endosome (11–13). Dendritic cell (DC) cross-priming of the TLR-mediated CTL response during microbial infection may not only upregulate costimulatory molecules but also regulate this process of cross-presentation (14–17). However, the molecular mechanisms of TLR-mediated cross-presentation remain unclear.

Lipidated peptides or proteins are promising vaccine candidates for inducing both humoral and cellular immune responses without conventional adjuvants (18–20). The use of synthetic lipopeptides as vaccines has many advantages, including ease of manufacture,

\*Graduate Institute of Life Sciences, National Defense Medical Center, Taipei 114, Taiwan; <sup>†</sup>National Institute of Infectious Diseases and Vaccinology, National Health Research Institutes, Miaoli County 350, Taiwan; and <sup>‡</sup>Graduate Institute of Immunology, China Medical University, Taichung 40402, Taiwan

Received for publication October 22, 2013. Accepted for publication February 27, 2014.

This work was supported by a grant from the National Health Research Institutes (IV-100-PP-04 to S.-J.L.) and a grant from the National Science Council (NSC 98-2320-B-400-011-MY3 to S.-J.L.).

K.-Y.S. performed the experiments, with contributions from Y.-C.S., I.-H.C., C.-H.L., H.-J.L., and P.C. and K.-Y.S., H.-W.C., and H.-J.L. analyzed the data. K.-Y.S. and S.-J.L. designed the experiments and wrote the manuscript.

Address correspondence and reprint requests to Prof. Shih-Jen Liu, National Institute of Infectious Diseases and Vaccinology, National Health Research Institutes, 35 Keyan Road, Zhunan Town, Miaoli County 350, Taiwan. E-mail address: levent@nhri.org.tw

The online version of this article contains supplemental material.

Abbreviations used in this article: BMDC, bone marrow-derived dendritic cell; DC, dendritic cell; EEA1, early endosome Ag-1; ER, endoplasmic reticulum; HPV16 E7, human papillomavirus type 16 E7; IDG, IDGPAGQAEPRAHYNIVTFCKCK; KO, knockout; LAMP1, lysosome-associated membrane protein-1; MFI, mean fluorescence intensity; Pam2EQL, Pam2-KSS-EQLESINFEKLTEWTSS<sub>253–270</sub>; Pam2IDG, Pam2-KSS-IDGPAGQAEPRAHYNIVTFCKCK; Rab7, RAS-related GTP-binding protein 7; RAH, RAHYNIVTF; WT, wild-type.

This article is distributed under The American Association of Immunologists, Inc., [Reuse Terms and Conditions for Author Choice articles](#).

Copyright © 2014 by The American Association of Immunologists, Inc. 0022-1767/14/\$16.00

biosafety, and low-cost vaccine development. In the past few decades, palmitoylated peptides containing cytotoxic or Th cell epitopes from tumor-associated Ags or viral proteins have shown the ability to induce strong antiviral and antitumor immunity (21, 22). For example, a lipopeptide containing the HBV core Ag peptide (aa 18–27), a tetanus toxoid peptide (aa 830–843), and two palmitic acids has been shown to induce CTL responses in humans (23). An HIV-1 lipopeptide vaccine, HIV-LIPO-5, which has also been used to immunize humans, elicits sustained Ag-specific CD4<sup>+</sup> and CD8<sup>+</sup> T cell immune responses (24–26). Additionally, a lipidated CTL epitope of human papillomavirus type 16 E7 (HPV16 E7) induced CTLs in cervical and vaginal cancer patients (27). These results indicate that the incorporation of a lipid moiety into Ags is a promising strategy for vaccine development. Recently, synthetic lipopeptides containing bacterial analogs were synthesized, and bacterial lipopeptides and lipoproteins have been identified as TLR2 agonists. However, the mechanisms of the presentation and processing of these lipopeptides for T cell activation are not clear.

In this study, we designed a dipalmitoylated lipopeptide (Pam2-KSS-IDGPAGQAEPDRAHYNIVTFCKKC, or Pam2IDG) from HPV16 E7 that contained an H-2D<sup>b</sup>-restricted CTL epitope (RAHYNIVTF, or RAH) to investigate the molecular mechanisms of TLR2-mediated cross-presentation and examine whether TLR2 signaling contributes to the regulation of intracellular cross-presentation.

## Materials and Methods

### Animals

C57BL/6 mice were purchased from the National Animal Center in Taiwan. TLR1-knockout (KO), TLR2KO, TLR6KO, and MyD88KO mice were purchased from Oriental Bioservice (Tokyo, Japan), and TAPKO mice were purchased from The Jackson Laboratory (Sacramento, CA). Additionally, OT-I (OVA-specific CD8<sup>+</sup> TCR-transgenic) mice were bred at the Laboratory Animal Center of the National Health Research Institutes (Miaoli, Taiwan). All of the animal studies were approved by the Institutional Animal Care and Use Committee of the National Health Research Institutes.

### Peptides and dipalmitic peptides

The peptides IDGPAGQAEPDRAHYNIVTFCKKC (IDG) and Pam2IDG, containing an H-2D<sup>b</sup>-restricted CTL epitope (amino acids 49–57; RAH) derived from the HPV16 E7 protein, were purchased from GL Biochem (Shanghai, China). Pam2-KSS-EQLESINFEKLTWSS<sub>253–270</sub> (Pam2EQL), which contains an H-2K<sup>b</sup>-restricted CTL epitope (aa 257–264; SIINFEKL), and IDG and Pam2IDG conjugated to FITC at a lysine residue were obtained from GeneDireX (Las Vegas, NV). These peptides were dissolved in DMSO at 10 mg/ml and stored at –20°C.

### Internalization of peptides

Bone marrow-derived DCs (BMDCs) were incubated with 1 μM Pam2IDG-FITC in complete RPMI 1640 medium at 37°C or 4°C for 15 min. To investigate the mechanisms of internalization, the BMDCs were pretreated with 2.5 μM filipin (Sigma-Aldrich) or 50 μM chlorpromazine (Sigma-Aldrich) for 30 min and then pulsed with Pam2IDG-FITC for 15 min. These BMDCs were harvested and stained with anti-CD11c-PE Ab for 20 min at 4°C. Pam2IDG-FITC internalization by CD11c<sup>+</sup> cells was then analyzed by flow cytometry.

### Animal tumor model

To establish an HPV16 E6/E7-expressing tumor model in C57BL/6 mice, we s.c. inoculated 2 × 10<sup>5</sup> TC-1 cells. To evaluate the therapeutic effect of peptide immunization, TC-1 tumor-bearing mice were immunized s.c. with PBS or 10 μg IDG or Pam2IDG in PBS on days 7 and 14. To investigate peptide cross-presentation by BMDCs, TC-1 tumor-bearing mice were immunized i.v. with PBS, BMDCs, or IDG- or Pam2IDG-pulsed BMDCs on day 7. The local tumor diameter was measured with calipers and monitored three times per week until 33–45 d. The tumor volume was calculated by the following formula: length × width × width/2.

### Laser scanning confocal microscopy

BMDCs were generated as previously described (20). To observe Pam2IDG internalization and localization, BMDCs were incubated with 1 μM FITC-conjugated Pam2IDG at 37°C. After incubation and washing away free peptides, the cells were fixed with 4% paraformaldehyde (Sigma-Aldrich) for 15 min at room temperature and then permeabilized in 0.1% saponin/PBS (eBioscience). After blocking with 3% BSA (Sigma-Aldrich) in PBS, the cells were stained with 5 μg/ml anti-early endosome Ag-1 (EEA1) (Abcam), anti-RAS-related GTP-binding protein 7 (Rab7; Rab7-117; Abcam), or anti-lysosome-associated membrane protein-1 (LAMP1; BioLegend) Ab for 1 h at room temperature. The cells were then washed with PBS and stained with 1 μg/ml Alexa Fluor 568-conjugated goat anti-rabbit IgG, Alexa Fluor 568-conjugated goat anti-mouse IgG, or Alexa Fluor 647-conjugated goat anti-rat IgG (Invitrogen, Eugene, OR). To detect H2-K<sup>b</sup>/OVA<sub>257–264</sub>, the cells were double stained with 5 μg/ml PE-conjugated 25.D1-16 Ab (eBioscience) and anti-Rab7 with secondary Ab 1 μg/ml Alexa Fluor 488-conjugated goat anti-mouse IgG. The cells were visualized using a Leica TCS SP5 II confocal microscope (Leica Microsystems, Heidelberg, Germany). Image processing and measurement of the colocalization rate were performed using Advanced Fluorescence software from Leica Microsystems. The formulas used for calculation were: colocalization rate = area of colocalization/area of foreground; and foreground = area of image/area of background.

### Western blotting

BMDCs were stimulated with 1 μM IDG or Pam2IDG for 0.5, 1, 2, or 3 h. The protein concentrations in the lysates were determined using a BCA Protein Assay Kit (Pierce, Rockford, IL). A total of 30 μg lysate was then electrophoresed on a 12% SDS-PAGE gel. After the resolved lysates in the gel were transferred to polyvinylidene difluoride membranes, the membranes were blocked with 5% milk in PBS containing 0.05% Tween-20. Next, the membranes were incubated with 1 μg/ml anti-Rab7 Ab (Abcam) in PBS containing 5% milk and 0.05% Tween-20 for 2 h at room temperature. An anti-GAPDH Ab was used as a loading control. The membranes were developed using the Luminata Crescendo Western HRP Substrate (Millipore, Billerica, MA). To inhibit MAPK activation, BMDCs were treated with 10 μM p38 inhibitor (SB203580; Calbiochem), 10 μM JNK inhibitor (Calbiochem), or 20 μM MEK inhibitor (PD98059; Sigma-Aldrich) for 30 min before pulsing with Pam2IDG.

### In vitro cross-presentation assay

To prepare the responders, mice were immunized twice with 30 μg RAH/IFA via s.c. injection on days 0 and 7. On day 14, CD8<sup>+</sup> T cells (purity >90%) were purified from the spleens by negative selection using a Dynabeads kit (Invitrogen). As the stimulators, BMDCs were pulsed with 1 μM IDG or Pam2IDG for 3 h and washed with complete RPMI 1640 medium. A total of 2 × 10<sup>4</sup> stimulators was then cocultured with 2 × 10<sup>5</sup> responders in anti-IFN-γ-coated ELISPOT plates for 48 h. IFN-γ-secreting cells were assessed by the ELISPOT assay. Moreover, to investigate the cross-presentation pathway of the dipalmitoylated peptides, 2 × 10<sup>5</sup> CD8<sup>+</sup> T cells (purity > 90%) were purified from OT-I splenocytes and cocultured with 2 × 10<sup>4</sup> Pam2EQL-pulsed BMDCs for 72 h. Thymidine incorporation was measured by adding 1 μCi/well [<sup>3</sup>H]thymidine for the last 18 h of culture and performing scintillation counting.

### Lentivirus preparation

Using the primers 5'-ATGACCTCTAGGAAGAAAGTGTG-3' and 5'-TCAACAACCTGCAGCTTTCTG-3', Rab7 was amplified from mouse cDNA and then cloned into a TA cloning vector (Invitrogen). For site-directed mutagenesis, the primers 5'-GGACTCTGGTGTGGAAAGAACTCTCTCATGAACAGTATGTG-3' and 5'-CACATACTGGTTCATGAGAGAGTTCTTCCAACACCAGAGTC-3' were used to clone the dominant-negative mutant Rab7T22N. Rab7 and Rab7T22N were cloned into the pLAS2w-Ppuro lentiviral vector (National RNAi Core Facility Platform, Taiwan, Republic of China) using the primers 5'-AAGCTAGCATGACCTCTAGGAAGAAAGTGTG-3' and 5'-AAACCGGT-TCAACAACCTGCAGCTTTCTGCGG-3'. Lentiviral vectors were produced by the cotransfection of 293FT cells (American Type Culture Collection) with three plasmids: 1) a vector plasmid (Rab7 or Rab7T22N); 2) the packaging plasmid pCMVΔR8.91; and 3) the envelope plasmid pMD.G. Lentiviral vector titration was then performed in A549 cells. These cells were infected with the lentiviral vector for 2 d, and viability was determined using an MTS assay (Promega, Madison, WI). The relative viability was assessed by comparison with uninfected wells (set as 100%). The relative infection unit was determined from the relative viability. Next, to overexpress Rab7, BMDCs were transfected with the lentiviral vector at

a multiplicity of infection of 5 with 5  $\mu\text{g/ml}$  polybrene in medium. Two days later, the lentiviral vector-transduced BMDCs were pulsed with 1  $\mu\text{M}$  Pam2EQL for the in vitro cross-presentation assay.

### Statistical analysis

Statistical significance was evaluated by a Student *t* test (two-tailed) at the 5% level.

## Results

### *TLR2 facilitates Pam2IDG endocytosis by BMDCs and is required for the tumor regression induced by Pam2IDG immunization*

To investigate TLR2-mediated endocytosis and Ag presentation, a dipalmitoylated lipopeptide (Pam2IDG) containing an H-2D<sup>b</sup>-restricted CTL epitope from HPV16 E7 was synthesized. The TLR2-stimulating activities of Pam2IDG were confirmed using BMDCs from wild-type (WT), TLR1KO, TLR2KO, and TLR6KO mice. The data showed that Pam2IDG, but not IDG, stimulated WT BMDCs to secrete TNF- $\alpha$  (Supplemental Fig. 1A). However, the stimulatory activity of Pam2IDG was lost when Pam2IDG was incubated with BMDCs from TLR2KO or TLR6KO mice (Supplemental Fig. 1B). We were thus interested in identifying whether TLR2 is involved in Ag presentation. To study the ability of TLR2 to facilitate the uptake of Pam2IDG, BMDCs from WT or TLR2KO mice were incubated with 1  $\mu\text{M}$  FITC-conjugated Pam2IDG at 4°C or 37°C for 30 min and then analyzed by flow cytometry. The internalization of Pam2IDG-FITC by WT BMDCs at 4°C was set as the background. Pam2IDG-FITC was taken up by the WT BMDCs during the 30 min incubation (mean fluorescence intensity [MFI]  $94.5 \pm 8$ ) at 37°C (Fig. 1A). In contrast, internalization of Pam2IDG-FITC was reduced in BMDCs from TLR2KO mice during 37°C incubation for 30 min (MFI  $81 \pm 1.5$ ). Similar results were obtained when anti-TLR2 Ab was used to block Pam2IDG-FITC internalization, and the MFI was reduced from 42.87 to 18.18 (Fig. 1B). These results indicate that TLR2 is an important receptor for Pam2IDG internalization. To further

identify the endocytosis pathway involved in Pam2IDG uptake, inhibitors (chlorpromazine or filipin) of clathrin- or caveola-mediated endocytosis were used in this study. BMDCs were pre-treated with 50  $\mu\text{M}$  chlorpromazine or 2.5  $\mu\text{M}$  filipin for 30 min and then coincubated with 1  $\mu\text{M}$  Pam2IDG-FITC for an additional 30 min at 37°C. We found that chlorpromazine completely inhibited the internalization of Pam2IDG-FITC (Fig. 1C), whereas filipin did not (Fig. 1D). This result indicates that the internalization of Pam2IDG by BMDCs is mediated by clathrin-dependent endocytosis rather than caveola-dependent endocytosis.

To examine whether endocytosed Pam2IDG could be presented by BMDCs and induce antitumor activity through TLR2, peptide-pulsed BMDCs from WT or TLR2KO mice were used to treat tumor-bearing mice. IDG- or Pam2IDG-pulsed BMDCs (IDG-BMDCs or Pam2IDG-BMDCs) from WT mice were i.v. injected into tumor-bearing mice (five per group) that had been inoculated s.c. 7 d beforehand with  $2 \times 10^5$  TC-1 cells. Tumor growth was then monitored every 2 to 3 d. As shown in Fig. 1E, tumor growth was inhibited in Pam2IDG-BMDC-treated mice but not in IDG-BMDC-treated or control mice (i.v. inoculated with PBS). The average tumor volume of the Pam2IDG-BMDC-treated mice was  $0.16 \pm 0.17 \text{ cm}^3$ , which was significantly smaller than the average tumor size of the IDG-BMDC group ( $0.74 \pm 0.14 \text{ cm}^3$ ) or the control group ( $1.46 \pm 0.42 \text{ cm}^3$ ) at 33 d postinoculation. The tumor size was also significantly smaller in IDG-BMDC-treated mice than in the control group ( $p < 0.001$ ). These data indicate that both IDG and Pam2IDG were cross-presented by BMDCs to induce antitumor immunity. Because the Pam2IDG-BMDCs had strong antitumor activity, we speculated that TLR2-mediated BMDC maturation or cross-presentation may contribute to antitumor immunity. To elucidate the role of TLR2, BMDCs from TLR2KO mice were used to investigate Pam2IDG-induced antitumor activity. Tumor regression was lost when tumors were treated with Pam2IDG-BMDCs from TLR2KO mice (Fig. 1E). Similarly, Pam2IDG-BMDCs from TLR6KO mice were unable to inhibit tumor growth (Supplemental Fig. 2A). These data provide

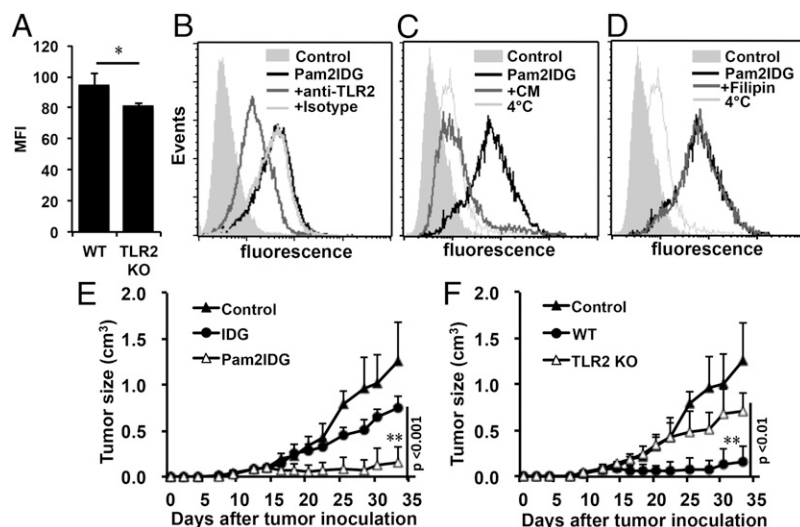


**FIGURE 1.** TLR2 was required for the endocytosis and cross-presentation of Pam2IDG in BMDCs. (A) WT or TLR2KO BMDCs were pulsed with 1  $\mu\text{M}$  FITC-conjugated Pam2IDG and incubated at 4°C or 37°C for 30 min. BMDCs that were not pulsed were used as controls. The results are shown as MFI value at 37°C, obtained by subtracting MFI at 4°C. Three independent experiments were performed. BMDCs were treated with 50  $\mu\text{g/ml}$  anti-TLR2 Ab or an isotype control Ab (B), 50  $\mu\text{M}$  chlorpromazine (CM) (C), or 2.5  $\mu\text{M}$  filipin (D) for 30 min and then coincubated with 1  $\mu\text{M}$  FITC-conjugated Pam2IDG for another 30 min. After free peptides were washed away, the cells were stained with anti-CD11c Ab. Data were collected by gating on CD11c<sup>+</sup> cells. Naive C57BL/6 mice (five per group) were inoculated with  $2 \times 10^5$  TC-1 tumor cells via s.c. injection before immunization. To examine the presentation of IDG and Pam2IDG, BMDCs were pulsed with 1  $\mu\text{M}$  peptides for 3 h. TC-1 tumor-bearing mice were immunized with PBS as a control group,  $2 \times 10^5$  IDG- or Pam2IDG-pulsed WT BMDCs (E), or  $2 \times 10^5$  Pam2IDG-pulsed WT or TLR2KO BMDCs (F) via i.v. injection at 7 d after tumor inoculation. Average tumor sizes are shown (cm<sup>3</sup>). The data are expressed as the mean  $\pm$  SD. \* $p < 0.05$ , \*\* $p < 0.01$ .

evidence indicating that TLR2/6 is necessary for the antitumor immunity induced by Pam2IDG-pulsed BMDCs. To further determine whether TLR2-mediated signaling is important for Pam2IDG-induced antitumor immunity, Pam2IDG-BMDCs from MyD88KO mice were used to treat tumor-bearing mice. We found that Pam2IDG-BMDCs from MyD88KO mice could not prevent tumor growth (Supplemental Fig. 2B). These results indicate that both cross-presentation and the TLR2-dependent activity of Pam2IDG contribute to Pam2IDG-mediated antitumor immunity. Therefore, a TLR2 agonist conjugated to an antigenic peptide may not only stimulate BMDC maturation but also facilitate TLR-mediated Ag cross-presentation by BMDCs to enhance Ag-specific antitumor immunity.

*The cross-priming mediated by TLR2 agonist-conjugated peptides is TAP independent*

Cross-presentation of exogenous Ag has been divided into two pathways: TAP dependent and TAP independent. TAP is required for reimporting peptides into the ER, phagosomes (28), or EEA1<sup>+</sup> endosomes (8). To determine whether TAP is necessary for the cross-presentation of Pam2IDG and the induction of CTL immune responses in vivo, Pam2IDG-pulsed BMDCs from WT or TAPKO mice were used to immunize mice. Surprisingly, Pam2IDG-pulsed TAPKO BMDCs induced  $12.45 \pm 3.7\%$  specific lysis, and Pam2IDG-pulsed WT BMDCs induced  $12.47 \pm 4.2\%$  specific lysis (Fig. 2A). These data indicate that TAP may not be essential for Pam2IDG cross-presentation. Next, TC-1 tumor-bearing mice (six per group) were immunized with  $2 \times 10^5$  Pam2IDG-pulsed WT or TAPKO BMDCs at day 7 postinoculation. We observed

that mice immunized with Pam2IDG-pulsed WT or TAPKO BMDCs had similar abilities to inhibit tumor growth. In particular, the average tumor volumes of mice treated with Pam2IDG-pulsed WT ( $0.15 \pm 0.42 \text{ cm}^3$ ) or TAPKO ( $0.01 \pm 0.02 \text{ cm}^3$ ) BMDCs were similar at day 40 post-tumor implantation (Fig. 2B). However, in the absence of Pam2IDG, the administration of WT or TAPKO BMDCs could not inhibit tumor growth; the average tumor volumes at day 40 were  $1.75 \pm 1.07$  and  $1.36 \pm 0.44 \text{ cm}^3$  in mice treated with WT or TAPKO BMDCs, respectively (Fig. 2B). These results suggest that Pam2IDG-mediated cross-presentation induces Ag-specific CTL responses and antitumor immunity via a TAP-independent pathway.

To further confirm the intracellular processing of Pam2IDG via a TAP-independent pathway, inhibitors of lysosomal acidification (chloroquine) and cathepsin S (Z-FL-COCHO) were used. BMDCs were incubated with  $25 \mu\text{M}$  chloroquine or  $5 \mu\text{M}$  Z-FL-COCHO at  $37^\circ\text{C}$  for 30 min. Because RAH bypasses Ag processing to bind to MHC class I molecules directly, we used RAH-pulsed BMDCs as a positive control to exclude BMDC damage caused by the inhibitors. After incubation, the BMDCs were pulsed with  $1 \mu\text{M}$  Pam2IDG or RAH for an additional 2.5 h. The inhibitor-treated BMDCs were then cocultured with responder cells ( $\text{CD8}^+$  T cells from RAH-immunized mice), and  $\text{IFN-}\gamma$  secretion was determined using an ELISPOT assay. As shown in Fig. 2C, chloroquine reduced the number of  $\text{IFN-}\gamma$ -secreting cells in the Pam2IDG-treated BMDC group ( $20 \pm 7$  versus  $102 \pm 17$ ) but not in the RAH-treated group (Fig. 2D). This result indicates that endosomal/lysosomal acidification is necessary for Pam2IDG-induced cross-priming. Similar results were observed for the

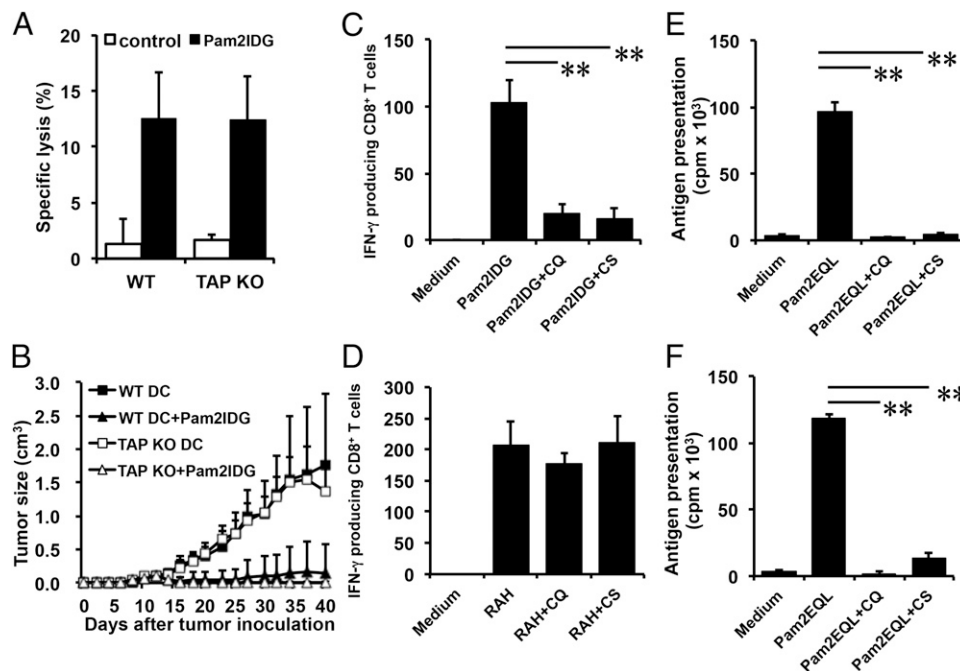


**FIGURE 2.** TLR2 agonist-conjugated peptides could be cross-presented by BMDCs via a TAP-independent pathway. BMDCs cultured from C57BL/6 WT or TAPKO mice were incubated with  $1 \mu\text{M}$  Pam2IDG for 3 h, and free peptides were then washed away. (A) Seven days after C57BL/6 mice were immunized with BMDCs via i.v. injection, the cytotoxic ability of Ag-specific T cells was assessed via an in vivo killing assay. The specific lysis percentages of the target cells were determined by flow cytometry. The data represent the average of two independent experiments. (B) TC-1 tumor-bearing mice (six per group) were immunized with  $2 \times 10^5$  peptide-pulsed BMDCs via i.v. injection. Average tumor sizes are shown ( $\text{cm}^3$ ). The data are expressed as the mean  $\pm$  SD. WT BMDCs were pretreated with  $25 \mu\text{M}$  chloroquine (CQ) or  $5 \mu\text{M}$  cathepsin S (CS) inhibitor for 30 min and then pulsed with  $1 \mu\text{M}$  Pam2IDG (C) or RAH (D) for 2.5 h at  $37^\circ\text{C}$ . After free peptides were washed away,  $2 \times 10^4$  BMDCs were cocultured for 48 h with  $2 \times 10^5$   $\text{CD8}^+$  T cells that were purified from the splenocytes of RAH/IFA-immunized mice.  $\text{IFN-}\gamma$ -secreting cells were then detected by an ELISPOT assay. WT (E) or TAPKO (F) BMDCs were pretreated as in (C) but pulsed with  $1 \mu\text{M}$  Pam2EQL for another 2.5 h at  $37^\circ\text{C}$ . After free peptides were washed away,  $2 \times 10^4$  BMDCs were cocultured for 48 h with  $2 \times 10^5$   $\text{CD8}^+$  T cells that were purified from OT-I splenocytes. Cell proliferation was determined using a [ $^3\text{H}$ ]thymidine incorporation assay. The data shown are representative of two independent experiments.  $**p < 0.01$ .

number of IFN- $\gamma$ -secreting cells stimulated by Z-FL-COCHO-treated BMDCs ( $15 \pm 8$ ). These data suggest that cathepsin S-dependent pathways are also important for Pam2IDG-induced cross-priming. To confirm that the cross-priming mechanisms are the same as for other TLR2 agonist-conjugated Ags, a dipalmitoylated peptide (Pam2EQL) containing an H-2K<sup>b</sup>-restricted OVA epitope (residues 257–264) was used as another model. Pam2EQL-pulsed BMDCs were pretreated with one of the inhibitors (chloroquine or Z-FL-COCHO) and then incubated with purified CD8<sup>+</sup> T cells from OT-I (OVA<sub>257–264</sub>-specific TCR-transgenic) mice. T cell proliferation was measured using the [<sup>3</sup>H]thymidine incorporation assay. Consistently, the cross-priming of Pam2EQL was blocked by both chloroquine and Z-FL-COCHO (Fig. 2E). In contrast, OT-I peptide-pulsed BMDCs still stimulated CD8<sup>+</sup> T cells in the presence of the inhibitors (Supplemental Fig. 3A). A similar result was obtained when BMDCs from TAPKO mice were used to stimulate T cell proliferation in the presence of one of the inhibitors (Fig. 2F, Supplemental Fig. 3B). To rule out the possibility that chloroquine and Z-FL-COCHO affect Pam2EQL-pulsed BMDC maturation, CD40 and CD86 expression on BMDCs was analyzed by flow cytometry. As the data show, chloroquine and Z-FL-COCHO did not impair Pam2EQL-pulsed BMDCs' maturation (Supplemental Fig. 4). These data suggest that TLR2 agonist-conjugated peptides may be cross-presented to T cells through a TAP-independent pathway.

#### *TLR2 agonist-conjugated peptides colocalize with Rab7<sup>+</sup> and LAMP1<sup>+</sup> endolysosomes*

An Ag can initially enter the early endosome via clathrin-mediated endocytosis and differentially traffic into the late endosome for Ag degradation or recycling to the plasma membrane (29). To efficiently prime CD8<sup>+</sup> T cells through Ag cross-presentation, an endocytosed Ag may escape from the endosome to the cytosol, or an Ag may be sorted into the endolysosome via the vacuolar pathway. To investigate the trafficking pathway of Pam2IDG, the localization of Pam2IDG and cellular compartments were analyzed by confocal microscopy. After BMDCs were incubated with 1  $\mu$ M FITC-conjugated IDG or Pam2IDG for 10, 20, or 30 min at 37°C, the cells were analyzed by laser scanning confocal microscopy. As shown in Fig. 3, IDG-FITC colocalized with the early endosome marker EEA1 (Fig. 3A), but not with Rab7<sup>+</sup> endosomes (Fig. 3B), between 10 and 30 min. In contrast, Pam2IDG-FITC colocalized with EEA1<sup>+</sup> endosomes at 10 min, but the colocalization was lower from 20–30 min (Fig. 3C), when Pam2IDG-FITC colocalized with Rab7<sup>+</sup> endosomes (Fig. 3D). The quantitative analysis is shown in Fig. 3E. IDG accumulated at EEA1<sup>+</sup> endosomes from 10–30 min (the colocalization rate was from  $42 \pm 8$  to  $71.2 \pm 5.1$ ). In contrast, Pam2IDG increased in colocalization with Rab7<sup>+</sup> endosomes until 30 min ( $39 \pm 4.6$ ) (Fig. 3F). The different localizations of IDG and Pam2IDG may reflect different processing mechanisms.

To further characterize the formation of peptide/MHC class I complexes in Rab7<sup>+</sup> endosomes or lysosomes, BMDCs were pulsed with 1  $\mu$ M Pam2EQL for 30 or 60 min and then stained with anti-Rab7 with secondary Ab Alexa Fluor 488-conjugated goat anti-mouse IgG or anti-LAMP1 with secondary Ab Alexa Fluor 647-conjugated goat anti-rat IgG. The mAb clone 25-D1.16 (30), which recognizes the H-2K<sup>b</sup>/OVA<sub>257–264</sub> complex, was used to detect this complex in Rab7<sup>+</sup> endosomes or lysosomes after Pam2EQL internalization. The H-2K<sup>b</sup>/OVA<sub>257–264</sub> complex was detected in either Rab7<sup>+</sup> endosomes or LAMP1<sup>+</sup> lysosomes (Fig. 3G). Moreover, the H-2K<sup>b</sup>/OVA<sub>257–264</sub> complex was found in Rab7<sup>+</sup> endosomes at 30 min and then in LAMP1<sup>+</sup> lysosomes at 60 min. These data suggest that internalized TLR2 ligand-conjugated

peptides are loaded onto MHC class I molecules in both Rab7<sup>+</sup> endosomes and LAMP1<sup>+</sup> lysosomes. In addition, we determined whether Pam2EQL internalization progressed from Rab7<sup>+</sup> endosomes to LAMP1<sup>+</sup> lysosomes in TAPKO BMDCs. We used the Ab 25-D1.16 to detect the H-2K<sup>b</sup>/OVA<sub>257–264</sub> complex in Pam2EQL-pulsed TAPKO BMDCs that were stained for either Rab7 or LAMP1. By confocal microscopy, we found that the H-2K<sup>b</sup>/OVA<sub>257–264</sub> complex colocalized with Rab7<sup>+</sup> endosomes and LAMP1<sup>+</sup> lysosomes in the TAPKO BMDCs (Fig. 3H). The localization patterns of the H-2K<sup>b</sup>/OVA<sub>257–264</sub> complex and the endosomal and lysosomal markers Rab7 and LAMP1, respectively, were more similar after 60 min than after 30 min. The patterns indicated that the TLR2 agonist-conjugated peptides were processed and formed the H-2K<sup>b</sup>/OVA<sub>257–264</sub> complex in the endolysosome. To avoid false-positive and -negative staining for 25D1.16, BMDCs from BALB/c (H-2<sup>d</sup>) or C57BL/6 (H-2<sup>b</sup>) mice were pulsed with Pam2EQL or Pam2IDG, respectively, prior to staining with 25D1.16 (PE). The cells were also stained with anti-Rab7 Ab or anti-LAMP1 Ab before staining with 25D1.16 (PE). Hence, nonspecific staining was not observed in our assay system (data not shown).

#### *TLR2 agonist-conjugated peptides upregulate Rab7 expression to promote cross-presentation*

Rab7<sup>+</sup> endosomes have been reported to sort Ags for degradation (29), and overexpression of Rab7 increases Ag presentation (31). However, whether Pam2IDG upregulates Rab7 expression through the TLR2/MyD88 pathway is unknown. To prove our hypothesis, Rab7 expression was detected in BMDCs incubated with IDG or Pam2IDG for 0, 0.5, 1, 2, or 3 h. The data showed that Rab7 expression in BMDCs was significantly upregulated by Pam2IDG but not by IDG (Fig. 4A). Accordingly, treatment of TLR2KO, TLR6KO, and MyD88KO BMDCs with Pam2IDG did not upregulate Rab7 expression (Fig. 4B, 4C). Previous studies showed TLR2 activation resulted in downstream MAPK signaling, such as JNK, p38, and ERK signaling (32, 33). To further investigate the signaling pathways of TLR2 that regulate Rab7 expression, MAPK signaling inhibitors were used to treat BMDCs. Cells lysates were collected from the MAPK inhibitor-treated BMDCs after pulsing with 1  $\mu$ M Pam2IDG for 0.5, 1, 2, and 3 h. Rab7 expression was then analyzed by Western blotting. Fig. 4D and 4F show that a JNK inhibitor and an MEK inhibitor (PD98059) impaired Pam2IDG-induced Rab7 expression in BMDCs, but a p38 inhibitor (SB203580) did not (Fig. 4E). These data suggest that Pam2IDG-induced Rab7 upregulation via TLR2/6/MyD88 and JNK and ERK signaling may aid Pam2IDG trafficking into Rab7<sup>+</sup> late endosomes/lysosomes for Ag processing.

To confirm our observation, BMDCs were transduced with Rab7 or Rab7T22N (an inactive mutant) using a lentiviral vector. After 2 d of transduction, the BMDCs were pulsed with Pam2EQL and then cocultured with OT-I CD8<sup>+</sup> T cells. Pam2EQL-pulsed Rab7-transduced BMDCs demonstrated increased Ag presentation compared with BMDCs alone or viral vector-transduced BMDCs, as measured by OT-I CD8<sup>+</sup> T cell proliferation (Fig. 5A). In contrast, Ag presentation was not increased in Pam2EQL-pulsed Rab7T22N-transduced BMDCs, as measured by OT-I CD8<sup>+</sup> T cell proliferation. Similar results were obtained using Pam2EQL-pulsed Rab7-transduced TAPKO BMDCs (Fig. 5B). We also monitored whether the lentiviral vector affected BMDC maturation. To further confirm whether the overexpression of Rab7 can increase the Ag presentation of nonlipidated peptide (EQL), lentiviral vector-transduced DCs were pulsed with 1  $\mu$ M EQL in an Ag presentation assay. We found that there was no significant difference between Rab7-transduced DCs and vector- or

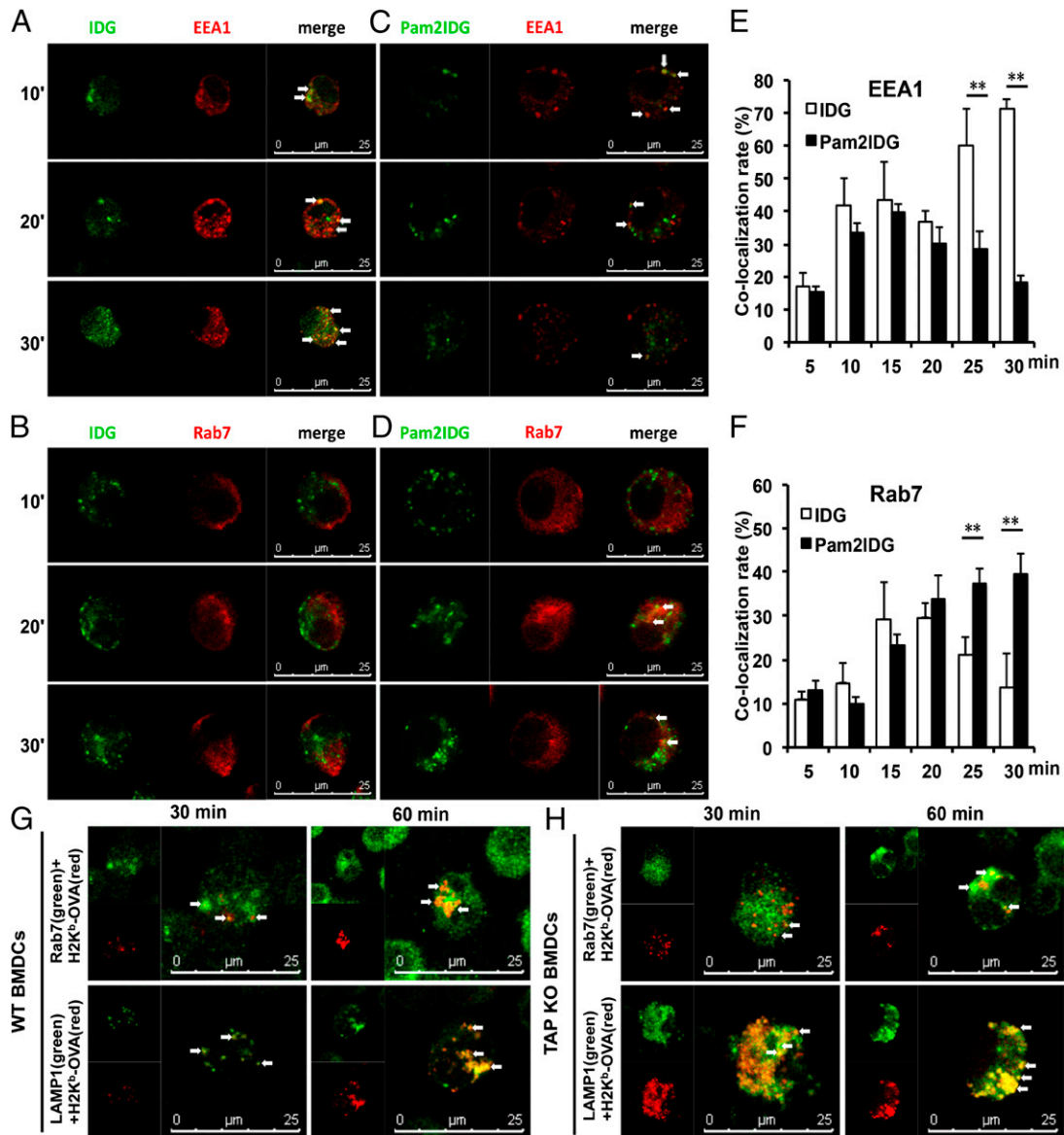


**FIGURE 3.** TLR2 agonist-conjugated peptides were internalized by Rab7<sup>+</sup> late endosomes and generated the epitope in endolysosomes. BMDCs were incubated with 1  $\mu$ M FITC-conjugated IDG or Pam2IDG (green) for 10, 20, or 30 min at 37°C. To detect endosomes, BMDCs were stained with anti-EEA1 (**A, C**) or anti-Rab7 (**B, D**) to visualize EEA1<sup>+</sup> and Rab7<sup>+</sup> endosomes (red), respectively. (**E** and **F**) The colocalization rates of IDG-FITC and Pam2IDG-FITC colocalized with EEA1<sup>+</sup> and Rab7<sup>+</sup> endosomes. WT (**G**) or TAPKO (**H**) BMDCs were incubated with 1  $\mu$ M Pam2EQL for 30 or 60 min. After incubation, the cells were double stained with 25.D1-16 Ab (red) to detect H2-K<sup>b</sup>/OVA<sub>257-264</sub> and with anti-Rab7 or anti-LAMP1 (green). Colocalization is depicted in yellow. The data shown are representative of two independent experiments. \*\**p* < 0.01.

Rab7T22N-transduced DCs in activating OT-I CD8<sup>+</sup> T cells (data not shown). Thus, the expression of Rab7 did not affect non-lipidated peptide presentation. These data indicate that the over-expression of Rab7 can enhance Pam2EQL cross-presentation by BMDCs via a TAP-independent pathway. In summary, upregulation of Rab7 expression partially explains how TLR2 agonist-conjugated peptides are efficiently presented to prime CD8<sup>+</sup> T cells via a TAP-independent pathway.

## Discussion

Synthetic lipopeptides with TLR2 activity have been validated as adjuvants to enhance immune responses (34–36). Furthermore, the incorporation of CTL epitopes into synthetic lipopeptides with TLR2 agonist activity has been shown to induce Ag-specific CD8<sup>+</sup> T cell responses (34, 37). However, there is limited information regarding the TLR2-mediated cross-priming of CTLs and its antitumor effects *in vivo*. In this report, we found that TLR2/MyD88

signaling was important for both TLR2-mediated cross-presentation and the antitumor effects of a synthetic diacylated lipopeptide. Moreover, we showed that Ag trafficking and processing in BMDCs were regulated by TLR2 activation via a TAP-independent pathway.

The internalization of Pam2IDG was completely dependent on clathrin-mediated endocytosis, indicating that this internalization occurs through receptor-mediated endocytosis. Although the internalization of Pam2IDG was reduced in TLR2KO BMDCs and by an anti-TLR2 Ab, we cannot exclude the possibility that unknown receptors may contribute to the endocytosis of Pam2IDG. In contrast to our findings, another group (38) found that the TLR2 ligand FSL-1 was internalized via a clathrin-dependent and TLR2-independent endocytosis pathway. Their data suggested that CD14 and CD36 were responsible for the internalization of FSL-1. In another study, the TLR2 agonist lipoteichoic acid was internalized through a clathrin-independent pathway in HEK/CD14 cells in the

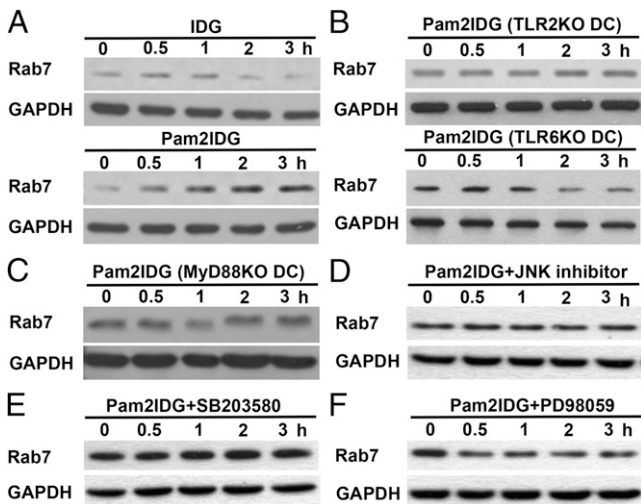


**FIGURE 4.** TLR2 agonist–conjugated peptides upregulated Rab7 expression via the TLR2–MyD88 pathway to enhance cross-presentation. (A) Lysates were collected from IDG- or Pam2IDG-treated WT BMDCs at the indicated time points. Lysates were collected from Pam2IDG-treated TLR2KO or TLR6KO (B), MyD88KO (C), JNK inhibitor– (D), SB203580– (E), or PD98059-treated (F) BMDCs at the indicated time points. Rab7 and GAPDH expression were then determined by Western blotting.

absence of TLR2 (39). Moreover, Pam3CysK4-conjugated lipopeptides activated APCs through TLR2, but the internalization of the Pam3CysK4-conjugated lipopeptide was independent of TLR2. Interestingly, both clathrin- and caveolin-mediated endocytosis were necessary for the conjugate’s endocytosis (37). Additionally, the different lipid structures of glycolipids with TLR2 agonist activity were found to be cross-presented by BMDCs using different intracellular pathways, but all required TLR2 (40). These studies did not have consistent conclusions regarding the internalization mechanisms of TLR2 agonist–conjugated Ags, so TLR2 may not be the only receptor responsible for the internalization of TLR2 agonists. Our results suggest that TLR2 plays an important role in the endocytosis of diacylated peptides.

After Ag internalization, the nonlipidated counterpart IDG was localized to EEA1<sup>+</sup> early endosomes but not Rab7<sup>+</sup> endosomes (Fig. 3A, 3B). We also found that IDG cross-presentation in BMDCs was TAP dependent (data not shown). Therefore, the cross-presentation mechanism of antigenic peptides without TLR2 agonist conjugation was more similar to that of soluble proteins proceeding through EEA1<sup>+</sup> early endosomes. In contrast to IDG, Pam2IDG colocalized with Rab7<sup>+</sup> endosomes. Most Rab7<sup>+</sup> endosomes have been reported to sort Ags for degradation (29), which may affect Ag cross-presentation. Vonderheit and Helenius (41) demonstrated that Semliki Forest virus is internalized by host cells through clathrin-mediated endocytosis and then internalized by Rab7<sup>+</sup> endosomes as cargo destined for the lysosome. To confirm our findings, another TLR2 agonist–conjugated peptide (Pam2EQL) was used to minimize the effect of the amino acid sequence and to allow peptide/MHC class I complex formation in the late endosome/lysosome. In this case, the H2-K<sup>b</sup>/OVA<sub>257–264</sub> complex was detected in Rab7<sup>+</sup> endosomes and LAMP1<sup>+</sup> lysosomes in BMDCs from both WT and TAPKO mice. The presentation of TLR2 agonist–conjugated peptides thus depends on the vacuolar pathway.

Triggering innate receptors is required to cross-present exogenous Ag to induce CD8<sup>+</sup> T cell priming. In addition to inducing cytokine secretion and the upregulation of costimulatory molecules, innate receptor signaling may also contribute to the regulation of cross-presentation. For example, TLR9 agonists have

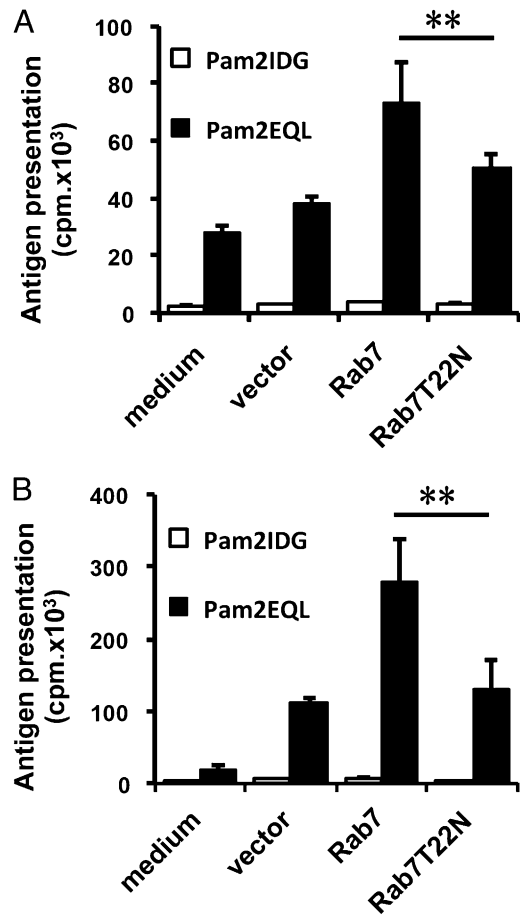


**FIGURE 5.** Rab7 overexpression could promote Pam2EQL cross-presentation by BMDCs. WT (A) or TAPKO (B) BMDCs were transduced with Lenti-vector, Lenti-Rab7, or Lenti-Rab7T22N for 2 d before being peptide pulsed. The transduced BMDCs were pulsed with 1  $\mu$ M Pam2IDG or Pam2EQL for 2.5 h at 37°C. After free peptides were washed away,  $2 \times 10^4$  BMDCs were cocultured for 48 h with  $2 \times 10^5$  CD8<sup>+</sup> T cells that were purified from the splenocytes of OT-I-transgenic mice. Cell proliferation was determined using a [<sup>3</sup>H]thymidine incorporation assay. The data shown are representative of two independent experiments. \*\**p* < 0.01.

been shown to increase TAP-independent Ag presentation by MHC class I (42). Moreover, TLR7 ligation limits Ag degradation in endophagosomal compartments and enhances the formation of peptide/MHC class I complexes on DCs (43). In this report, we further investigated whether the endosomal-associated protein Rab7 could be upregulated by TLR2 ligation. The overexpression of Rab7 has been shown to enhance Ag presentation by MHC class II molecules on B cells (31). Conversely, Boes et al. (44) have reported that innate signaling remodels the late endosomal compartment for MHC class II peptide loading. Our data suggest that Rab7 is upregulated by the TLR2 agonist Pam2IDG, leading to the efficient trafficking of Pam2IDG from the early endosome to the late endosome/lysosome for loading onto MHC class I molecules. A similar observation was made using Pam2EQL as a model. Moreover, the engagement of TLR2 led to the activation of multiple signaling pathways in DCs, including JNK, p38, ERK, MyD88, and NF- $\kappa$ B signaling (32, 33). Our data showed that the upregulation of Rab7 is dependent on MyD88 pathway (Fig. 4C). Because MyD88 controls the activation of MAPKs such as JNK, p38, and ERK, activation of different signaling pathways may have different functions. Fig. 4D–F further indicate that JNK and ERK are necessary for TLR2-mediated upregulation of Rab7. Similarly, several studies have demonstrated that ERK regulates

intracellular endocytotic traffic (45–47). Fang et al. (48) also reported TLR2-mediated phagocytosis and autophagy through the JNK signaling pathway in macrophages. Another recent study has shown that IL-12-mediated activation of p38 MAPK induces the expression of Rab7 to regulate endocytic trafficking (49). In contrast, our results have shown that TLR2-mediated activation of JNK and ERK induces the expression of Rab7, which facilitates Ag traffic to the late endosome/lysosome for efficient Ag presentation to CD8<sup>+</sup> T cells. These results reveal that endosomal traffic can be regulated by different receptors or by MAPK signaling pathway. Our findings thus explore the possible link between innate signaling and the Rab7<sup>+</sup> endosomal pathway in Ag cross-presentation.

In conclusion, our study provides evidence indicating that TLR2 agonist-conjugated Ags are endocytosed via a clathrin-dependent pathway and cross-presented via a TAP-independent vesicular pathway through the upregulation of the protein Rab7.

## Acknowledgments

We thank Johns Hopkins University for providing the TC-1 cells.

## Disclosures

The authors have no financial conflicts of interest.

## References

- Flinsberg, T. W., E. B. Compeer, J. J. Boelens, and M. Boes. 2011. Antigen cross-presentation: extending recent laboratory findings to therapeutic intervention. *Clin. Exp. Immunol.* 165: 8–18.
- Monu, N., and E. S. Trombetta. 2007. Cross-talk between the endocytic pathway and the endoplasmic reticulum in cross-presentation by MHC class I molecules. *Curr. Opin. Immunol.* 19: 66–72.
- Guermonez, P., L. Saveanu, M. Kleijmeer, J. Davoust, P. Van Endert, and S. Amigorena. 2003. ER-phagosome fusion defines an MHC class I cross-presentation compartment in dendritic cells. *Nature* 425: 397–402.
- Shen, L., L. J. Sigal, M. Boes, and K. L. Rock. 2004. Important role of cathepsin S in generating peptides for TAP-independent MHC class I cross-presentation in vivo. *Immunity* 21: 155–165.
- Shen, L., and K. L. Rock. 2006. Priming of T cells by exogenous antigen cross-presented on MHC class I molecules. *Curr. Opin. Immunol.* 18: 85–91.
- Firat, E., L. Saveanu, P. Aichele, P. Staeheli, J. Huai, S. Gaedicke, A. Nil, G. Besin, B. Kanzler, P. van Endert, and G. Niedermann. 2007. The role of endoplasmic reticulum-associated aminopeptidase 1 in immunity to infection and in cross-presentation. *J. Immunol.* 178: 2241–2248.
- Merzougui, N., R. Kratzer, L. Saveanu, and P. van Endert. 2011. A proteasome-dependent, TAP-independent pathway for cross-presentation of phagocytosed antigen. *EMBO Rep.* 12: 1257–1264.
- Burgdorf, S., C. Schölz, A. Kautz, R. Tampé, and C. Kurts. 2008. Spatial and mechanistic separation of cross-presentation and endogenous antigen presentation. *Nat. Immunol.* 9: 558–566.
- Kovacsics-Bankowski, M., and K. L. Rock. 1995. A phagosome-to-cytosol pathway for exogenous antigens presented on MHC class I molecules. *Science* 267: 243–246.
- Mant, A., F. Chinnery, T. Elliott, and A. P. Williams. 2012. The pathway of cross-presentation is influenced by the particle size of phagocytosed antigen. *Immunology* 136: 163–175.
- Chatterjee, B., A. Smed-Sörensen, L. Cohn, C. Chalouni, R. Vandlen, B. C. Lee, J. Widger, T. Keler, L. Delamarre, and I. Mellman. 2012. Internalization and endosomal degradation of receptor-bound antigens regulate the efficiency of cross presentation by human dendritic cells. *Blood* 120: 2011–2020.
- Tacke, P. J., W. Ginter, L. Berod, L. J. Cruz, B. Joosten, T. Sparwasser, C. G. Figdor, and A. Cambi. 2011. Targeting DC-SIGN via its neck region leads to prolonged antigen residence in early endosomes, delayed lysosomal degradation, and cross-presentation. *Blood* 118: 4111–4119.
- Delamarre, L., M. Pack, H. Chang, I. Mellman, and E. S. Trombetta. 2005. Differential lysosomal proteolysis in antigen-presenting cells determines antigen fate. *Science* 307: 1630–1634.
- Wagner, C. S., and P. Cresswell. 2012. TLR and nucleotide-binding oligomerization domain-like receptor signals differentially regulate exogenous antigen presentation. *J. Immunol.* 188: 686–693.
- de Brito, C., M. Tomkowiak, R. Ghittoni, C. Caux, Y. Leverrier, and J. Marvel. 2011. CpG promotes cross-presentation of dead cell-associated antigens by pre-CD8 $\alpha$ <sup>+</sup> dendritic cells [corrected]. *J. Immunol.* 186: 1503–1511.
- Oh, J. Z., and R. M. Kedl. 2010. The capacity to induce cross-presentation dictates the success of a TLR7 agonist-conjugate vaccine for eliciting cellular immunity. *J. Immunol.* 185: 4602–4608.
- Simmons, D. P., D. H. Canaday, Y. Liu, Q. Li, A. Huang, W. H. Boom, and C. V. Harding. 2010. *Mycobacterium tuberculosis* and TLR2 agonists inhibit induction of type I IFN and class I MHC antigen cross processing by TLR9. *J. Immunol.* 185: 2405–2415.
- Gahéry-Ségard, H., G. Pialoux, B. Charmeteau, S. Sermet, H. Poncelet, M. Raux, A. Tartar, J. P. Lévy, H. Gras-Masse, and J. G. Guillet. 2000. Multi-epitopic B- and T-cell responses induced in humans by a human immunodeficiency virus type 1 lipopeptide vaccine. *J. Virol.* 74: 1694–1703.
- Andrieu, M., E. Loing, J. F. Desoutter, F. Connan, J. Choppin, H. Gras-Masse, D. Hanau, A. Dautry-Varsat, J. G. Guillet, and A. Hosmalin. 2000. Endocytosis of an HIV-derived lipopeptide into human dendritic cells followed by class I-restricted CD8(+) T lymphocyte activation. *Eur. J. Immunol.* 30: 3256–3265.
- Chen, H.-W., S.-J. Liu, H.-H. Liu, Y. Kwok, C.-L. Lin, L.-H. Lin, M.-Y. Chen, J.-P. Tsai, L.-S. Chang, F.-F. Chiu, et al. 2009. A novel technology for the production of a heterologous lipoprotein immunogen in high yield has implications for the field of vaccine design. *Vaccine* 27: 1400–1409.
- Xu, D. H., C. H. Zhou, Y. P. Xia, Z. Y. Qiu, Y. Z. Wu, Z. C. Jia, and W. Zhou. 2007. Cytotoxic T lymphocyte response induced by an improved synthetic lipopeptide vaccine against cervical cancer. *Acta Pharmacol. Sin.* 28: 695–702.
- Baz, A., K. Buttigieg, W. Zeng, M. Rizkalla, D. C. Jackson, P. Groves, and A. Kelso. 2008. Branched and linear lipopeptide vaccines have different effects on primary CD4<sup>+</sup> and CD8<sup>+</sup> T-cell activation but induce similar tumor-protective memory CD8<sup>+</sup> T-cell responses. *Vaccine* 26: 2570–2579.
- Vitiello, A., G. Ishioka, H. M. Grey, R. Rose, P. Farness, R. LaFond, L. Yuan, F. V. Chisari, J. Furze, R. Bartholomeuz, et al. 1995. Development of a lipopeptide-based therapeutic vaccine to treat chronic HBV infection. I. Induction of a primary cytotoxic T lymphocyte response in humans. *J. Clin. Invest.* 95: 341–349.
- Salmon-Céron, D., C. Durier, C. Desaint, L. Cuzin, M. Surenaud, N. B. Hamouda, J. D. Lelièvre, B. Bonnet, G. Pialoux, I. Poizat-Martin, et al. ANRS VAC18 trial group. 2010. Immunogenicity and safety of an HIV-1 lipopeptide vaccine in healthy adults: a phase 2 placebo-controlled ANRS trial. *AIDS* 24: 2211–2223.
- Pialoux, G., R. P. Quercia, H. Gahery, N. Daniel, L. Slama, P. M. Girard, P. Bonnard, W. Rozenbaum, V. Schneider, D. Salmon, and J. G. Guillet. 2008. Immunological responses and long-term treatment interruption after human immunodeficiency virus type 1 (HIV-1) lipopeptide immunization of HIV-1-infected patients: the LIPHTHERA study. *Clin. Vaccine Immunol.* 15: 562–568.
- Gahery, H., S. Figueiredo, C. Texier, S. Pouvell-Moratille, L. Ourth, C. Igea, M. Surenaud, J. G. Guillet, and B. Maillere. 2007. HLA-DR-restricted peptides identified in the Nef protein can induce HIV type 1-specific IL-2/IFN-gamma-secreting CD4<sup>+</sup> and CD4<sup>+</sup>/CD8<sup>+</sup> T cells in humans after lipopeptide vaccination. *AIDS Res. Hum. Retroviruses* 23: 427–437.
- Steller, M. A., K. J. Gurski, M. Murakami, R. W. Daniel, K. V. Shah, E. Celis, A. Sette, E. L. Trimble, R. C. Park, and F. M. Marincola. 1998. Cell-mediated immunological responses in cervical and vaginal cancer patients immunized with a lipidated epitope of human papillomavirus type 16 E7. *Clin. Cancer Res.* 4: 2103–2109.
- Houde, M., S. Bertholet, E. Gagnon, S. Brunet, G. Goyette, A. Laplante, M. F. Princiotto, P. Thibault, D. Sacks, and M. Desjardins. 2003. Phagosomes are competent organelles for antigen cross-presentation. *Nature* 425: 402–406.
- Lakadamyali, M., M. J. Rust, and X. Zhuang. 2006. Ligands for clathrin-mediated endocytosis are differentially sorted into distinct populations of early endosomes. *Cell* 124: 997–1009.
- Porgador, A., J. W. Yewdell, Y. Deng, J. R. Bennink, and R. N. Germain. 1997. Localization, quantitation, and in situ detection of specific peptide-MHC class I complexes using a monoclonal antibody. *Immunity* 6: 715–726.
- Bertram, E. M., R. G. Hawley, and T. H. Watts. 2002. Overexpression of rab7 enhances the kinetics of antigen processing and presentation with MHC class II molecules in B cells. *Int. Immunol.* 14: 309–318.
- Farhat, K., S. Riekenberg, H. Heine, J. Debarry, R. Lang, J. Mages, U. Buwitt-Beckmann, K. Röschmann, G. Jung, K. H. Wiesmüller, and A. J. Ulmer. 2008. Heterodimerization of TLR2 with TLR1 or TLR6 expands the ligand spectrum but does not lead to differential signaling. *J. Leukoc. Biol.* 83: 692–701.
- Leng, C. H., H. W. Chen, L. S. Chang, H. H. Liu, H. Y. Liu, Y. P. Sher, Y. W. Chang, S. P. Lien, T. Y. Huang, M. Y. Chen, et al. 2010. A recombinant lipoprotein containing an unsaturated fatty acid activates NF- $\kappa$ B through the TLR2 signaling pathway and induces a differential gene profile from a synthetic lipopeptide. *Mol. Immunol.* 47: 2015–2021.
- Prajeeth, C. K., A. C. Jirmo, J. K. Krishnaswamy, T. Ebensen, C. A. Guzman, S. Weiss, H. Constabel, R. E. Schmidt, and G. M. N. Behrens. 2010. The synthetic TLR2 agonist BPPeysMPEG leads to efficient cross-priming against co-administered and linked antigens. *Eur. J. Immunol.* 40: 1272–1283.
- Nguyen, D. T., L. de Witte, M. Ludlow, S. Yüksel, K. H. Wiesmüller, T. B. Geijtenbeek, A. D. Osterhaus, and R. L. de Swart. 2010. The synthetic bacterial lipopeptide Pam3CSK4 modulates respiratory syncytial virus infection independent of TLR activation. *PLoS Pathog.* 6: e1001049.
- Kiura, K., H. Kataoka, T. Nakata, T. Into, M. Yasuda, S. Akira, N. Inoue, and K. Shibata. 2006. The synthetic analogue of mycoplasma lipoprotein FSL-1 induces dendritic cell maturation through Toll-like receptor 2. *FEMS Immunol. Med. Microbiol.* 46: 78–84.
- Khan, S., M. S. Bijker, J. J. Weterings, H. J. Tanke, G. J. Adema, T. van Hall, J. W. Drijfhout, C. J. Melief, H. S. Overkleef, G. A. van der Marel, et al. 2007. Distinct uptake mechanisms but similar intracellular processing of two different toll-like receptor ligand-peptide conjugates in dendritic cells. *J. Biol. Chem.* 282: 21145–21159.
- Shamsul, H. M., A. Hasebe, M. Iyori, M. Ohtani, K. Kiura, D. Zhang, Y. Totsuka, and K. Shibata. 2010. The Toll-like receptor 2 (TLR2) ligand FSL-1



- is internalized via the clathrin-dependent endocytic pathway triggered by CD14 and CD36 but not by TLR2. *Immunology* 130: 262–272.
39. Triantafilou, M., M. Manukyan, A. Mackie, S. Morath, T. Hartung, H. Heine, and K. Triantafilou. 2004. Lipoteichoic acid and toll-like receptor 2 internalization and targeting to the Golgi are lipid raft-dependent. *J. Biol. Chem.* 279: 40882–40889.
  40. Renaudet, O., G. Dasgupta, I. Bettahi, A. Shi, A. B. Nesburn, P. Dumy, and L. BenMohamed. 2010. Linear and branched glyco-lipopeptide vaccines follow distinct cross-presentation pathways and generate different magnitudes of anti-tumor immunity. *PLoS ONE* 5: e11216.
  41. Vonderheit, A., and A. Helenius. 2005. Rab7 associates with early endosomes to mediate sorting and transport of Semliki forest virus to late endosomes. *PLoS Biol.* 3: e233.
  42. Chen, L., and M. Jondal. 2009. TLR9 activation increases TAP-independent vesicular MHC class I processing in vivo. *Scand. J. Immunol.* 70: 431–438.
  43. Crespo, M. I., E. R. Zacca, N. G. Núñez, R. P. Ranocchia, M. Maccioni, B. A. Maletto, M. C. Pistoiresi-Palencia, and G. Morón. 2013. TLR7 triggering with polyuridylic acid promotes cross-presentation in CD8 $\alpha$ + conventional dendritic cells by enhancing antigen preservation and MHC class I antigen permanence on the dendritic cell surface. *J. Immunol.* 190: 948–960.
  44. Boes, M., J. Cerny, R. Massol, M. Op den Brouw, T. Kirchhausen, J. Chen, and H. L. Ploegh. 2002. T-cell engagement of dendritic cells rapidly rearranges MHC class II transport. *Nature* 418: 983–988.
  45. Galperin, E., and A. Sorkin. 2008. Endosomal targeting of MEK2 requires RAF, MEK kinase activity and clathrin-dependent endocytosis. *Traffic* 9: 1776–1790.
  46. Teis, D., N. Taub, R. Kurzbauer, D. Hilber, M. E. de Araujo, M. Erlacher, M. Offterdinger, A. Villunger, S. Geley, G. Bohn, et al. 2006. p14-MP1-MEK1 signaling regulates endosomal traffic and cellular proliferation during tissue homeostasis. *J. Cell Biol.* 175: 861–868.
  47. Robertson, S. E., S. R. Setty, A. Sitaram, M. S. Marks, R. E. Lewis, and M. M. Chou. 2006. Extracellular signal-regulated kinase regulates clathrin-independent endosomal trafficking. *Mol. Biol. Cell* 17: 645–657.
  48. Fang, L., H. M. Wu, P. S. Ding, and R. Y. Liu. 2014. TLR2 mediates phagocytosis and autophagy through JNK signaling pathway in *Staphylococcus aureus*-stimulated RAW264.7 cells. *Cell. Signal.* 26: 806–814.
  49. Bhattacharya, M., N. Ojha, S. Solanki, C. K. Mukhopadhyay, R. Madan, N. Patel, G. Krishnamurthy, S. Kumar, S. K. Basu, and A. Mukhopadhyay. 2006. IL-6 and IL-12 specifically regulate the expression of Rab5 and Rab7 via distinct signaling pathways. *EMBO J.* 25: 2878–2888.